A Dynamic Array Using Spatial Amplitude Modulation with an Asymmetric Wilkinson Power Divider for Secure Wireless Applications

Jacob R. Randall, *Graduate Student Member, IEEE*, Amer Abu Arisheh, *Graduate Student Member, IEEE*, Jason M. Merlo, *Graduate Student Member, IEEE*, and Jeffrey A. Nanzer, *Senior Member, IEEE*

***Abstract*—A new method of obtaining directional modulation by implementing antenna array dynamics is proposed. An asymmetric switching feed structure is implemented in a two-element array that supports a static antenna pattern in a desired direction while adding sufficient complex modulation at other angles to mitigate the transfer of information. The dynamic antenna array feeds are calibrated to be in-phase and have a signal feed amplitude ratio of approximately 6.15 $\pm$ 0.1 dB through the design of an asymmetrical Wilkinson divider. The antenna system comprises of a two-state switching matrix using a double pole double throw (DPDT) RF switch. Secure communication capability is demonstrated in simulation and experiment by a 2.5 GHz two-element patch array. The communication system uses a 16-QAM single-carrier signal transmitting 48 kbits in a pseudo-random bit sequence (PRBS) at a rate of 4 Mbits/s. The DPDT switch was synchronized to the transmitter symbol rate of 1 MHz. To isolate the effects of the phase dynamics, the communication system was operating at an SNR of 33 dB, thus transmitting high power to all directions. A low bit error ratio (BER) of $< 10^{-3}$ is demonstrated at the desired transmission direction $\phi \leq |13^{\circ}|$, with higher BER outside this region. A measurement of a static antenna yielded BER $= 0$ in all directions; thus, the bit errors and narrow $\pm 13^{\circ}$ information beamwidth were due exclusively to the antenna array dynamics. Performance metrics of this directional modulation technique are compared against previous literature for the reader. Further insights to spurious signals and mitigation are taken into consideration for the equipment and instrumentation of a narrowband signal to validate the technique as a viable "black-box" system implementation.**

***Index Terms*—Distributed array, dynamic arrays, dynamic antennas, directional modulation, secure wireless**

I. Introduction

Security at the physical layer is emerging as an integral aspect of wireless communication. As an increasing number of devices with wireless communications and wireless sensors enter the market, the potential for malicious and unintentional interference from other devices will become a concern that must be addressed to ensure safe and acceptable wireless system performance for a range of applications [1]–[3]. While higher-level key-based cryptography methods have long been integrated into communications systems, the inclusion of physical layer security will help ensure that future wireless systems are robust to interference and malicious actions. The low-level physical layer encryption methodology referred to as directional modulation (DM) has been studied for its effectiveness in maintaining low bit errors in a narrow secure spatial region while increasing bit errors elsewhere. Previous DM methods include a near-field parasitic element switching based modulation [4], a switching scheme to maximize BER in undesired directions by combinatorial interference [5], which is based on vector synthesis analysis of DM transmitter designs [6], and phase vector control of a two-element array using a phase shifter [7]. However, many of these methods involve complicated architectures implemented with electrically large arrays and do not maintain optimal main beam gain [8]. Phased array methods have been demonstrated [9], [10], as well as methods using use spatial dynamics [11], which offer more power-efficient solutions. While array gain is maintained in [11], the use of physical motion to implement directional modulation may limit the effective data rates of systems. To address the challenges of obtaining DM in a simple architecture with a small aperture, without physical motion, and without turning off radiating elements, directional modulation with a single element has been demonstrated [12] as well as two-element antenna array excited by a single pole double throw (SPDT) RF switch [13] which provide theoretical insights to spatial amplitude dynamics. The switching structure provided time varying phase dynamics and constant transmitted power. This concept is limited to using only half of the aperture since only one antenna is used at a time, thus widening the beamwidth, reducing the power density at the desired transmission angle, and not being capable of beamsteering.

We present a novel approach to physical layer wireless security using a dynamic antenna that switches rapidly at the information rate using spatial amplitude dynamics. In contrast to reconfigurable antenna systems, which use switching to find and maintain a feasible antenna state, our dynamic antenna concept relies on rapid changes in the antenna system. A two-element 2.5 GHz antenna with asymmetric input amplitudes is designed, and the inputs signals are switched to create an antenna pattern that is dynamic in space and time. While the overall radiated power does not change, the relative amplitude changes, altering the apparent location of the antenna and resulting in phase dynamics in the radiated fields. Higher overall gain is maintained compared to other

Manuscript received 2023.

This work was supported in part by the National Science Foundation under Grant #2028736. *(Corresponding author: Jeffrey A. Nanzer)*

The authors are with the Department of Electrical and Computer Engineering, Michigan State University, East Lansing, MI 48824 USA (email: randa130@msu.edu, abuarish@msu.edu, merlojas@msu.edu, nanzer@msu.edu.

switched antenna systems since both antennas are always in use and the total radiated power is unchanged. While prior work has explored changing the current distribution on a single element [12], this work demonstrates the feasibility of using dynamics in two-element structures by changing only the excitation signal amplitudes. We design and experimentally demonstrate a two-element antenna using an asymmetric Wilkinson power divider and a double pole double throw (DPDT) RF switch to rapidly switch the asymmetric signal feeds. We demonstrate the ability to maintain a constant antenna pattern in a narrow angular region while using dynamics to add additional modulation at angles outside the information beamwidth (IB). We experimentally demonstrate the use of the dynamic antenna in a wireless communications system and show that a narrow information beamwidth is obtained for 16-QAM modulation. A measurement of a static antenna yielded no bit errors (BER $= 0$) across all angles; thus, all bit errors were due exclusively to the antenna array dynamics.

II. Dynamic Two-Element Antenna

The dynamic antenna is based on a two-element antenna system with asymmetric signal power fed to each antenna. The signal power at each antenna is modulated at a rate equal to that of the information being transmitted or received by the array, thus generating a dynamic radiation pattern. The array factor of the two-element array can be given by

$$AF(\theta,t) = \alpha(t)e^{-j\frac{kd}{2}\sin\theta} + [1-\alpha(t)]\,e^{j\frac{kd}{2}\sin\theta} \quad (1)$$

where $\alpha(t)$ is a dynamic amplitude weight, $k = 2\pi/\lambda$ with λ the wavelength of the carrier frequency, d is the antenna baseline, and θ is the observation angle defined relative to the direction broadside to the array baseline vector. In a static array, the amplitude weight $\alpha(t)$ would be a constant. In this work, we rapidly vary $\alpha(t)$ between two amplitude values, generating the dynamic array factor. The amplitude in this work is given by

$$\alpha(t) = \begin{cases} a, & (n-1)\,T_0 < t < \left(n-\frac{1}{2}\right)T_0 \\ 1-a, & \left(n-\frac{1}{2}\right)T_0 < t < nT_0 \end{cases} \quad (2)$$

where $0 \le a \le 1$, T_0 is the switching period, which in this work is equal to the symbol rate of the information transmitted by the antenna, and n is an integer. The amplitude ratio between the two elements can be given by $10\log_{10}\left[\frac{\alpha(t)}{1-\alpha(t)}\right]$. The magnitude of the array factor is

$$|AF(\theta)| = \left[a^2 + (1-a)^2 + a(1-a)\cos\left(kd\cos\phi\right)\right]^{-\frac{1}{2}} \quad (3)$$

and the phase is

$$\angle AF(\phi) = \tan^{-1}\left[\left(\frac{a-(1-a)}{a+(1-a)}\right)\tan\left(\frac{kd}{2}\cos\phi\right)\right] \quad (4)$$

When the dynamic antenna transitions between states, i.e. $a \to (1-a)$ and vice versa, the magnitude (3) is unchanged. The phase (4), however, undergoes a sign change at all angles except $\phi = 90°$. A differential phase occurs at all angles away from broadside. The dynamic antenna switches between two states (referred to as state 1 and state 2), where the antenna amplitudes $[\alpha(t), 1-\alpha(t)]$ are given by $[a, 1-a]$ (state 1) and $[1-a, a]$ (state 2). The amplitude imbalance changes the apparent electrical location of the antenna, thus by switching between the two states different radiated phase pattern is obtained.

The dynamic antenna was fabricated using a two-element microstrip patch array fed by an asymmetric Wilkinson power divider, the outputs of which were dynamically switched using a DPDT switch, as shown in Fig. 1. The antennas were designed at 2.5 GHz and modeled in HFSS. Each probe-fed patch antenna was designed to operate at 2.5 GHz and had a width of 29.95 mm and a length of 39.28 mm. The antennas were printed on Rogers RO4350B substrate material with a substrate thickness of 1.542 mm. The ground plane under the antenna was made larger than the edges of the antennas by at least $\lambda/4$ on each side for a total length of 181 mm and width of 99.5 mm. The feed point was then designed to impedance match the antenna to 50 Ω, which was obtained with a feed location of 9.6 mm from the edge of the patch. The simulated gain of the antenna was 5.74 dBi. A 1×2 array was then designed in HFSS. A 6.15 dB amplitude ratio between the signal feeds was implemented, which achieved a total array gain of 7.56 dBi in either state.

The feeding system is based on an asymmetric Wilkinson power divider that yields a 6.15 ± 0.1 dB amplitude ratio between the two feeds of the antennas [14], [15]. A DPDT switch is used to rapidly change the signal path of the feeds. The Wilkinson power divider was manufactured on a Rogers RO4350B substrate with height of 1.542 mm. The isolation resistor of the Wilkinson power divider was a 113 Ω resistor. The S11, S22, and S33 parameters were –12.5 dB, –22.0 dB, and –7.22 dB, respectively. The Wilkinson divider has an isolation of 9.31 dB, an S12 of –1.08 dB, and an S13 of –7.23 dB. Thus, the amplitude ratio is 6.15 dB. The fabricated Wilkinson power divider is shown in Fig. 2. The added losses from the Wilkinson divider are not considered due to the need for a feeding network in a traditional array. The active DPDT RF switch is a Skyworks Solutions SKY13411-374LF-EVB. The loss from the DPDT switch is due to 0.6 dB of insertion loss at 2.5GHz and 0.26 dB of losses due to switching DC blocking capacitors on the switch evaluation board.

The communication system transmitted 48 kbits in 16-QAM configured pseudo-random sequences. Switching was applied to the received signal while synchronized to the symbol rate of the communication signal. The QAM signal is received by the dynamic antenna array elements, each of which passes through the DPDT switch and the Wilkinson divider, then the combined signal arrives at the receiver and is compared against the original transmitted signal. The switch was driven with two 3.3 V logic control signals from a Teensy 4.0 microcontroller (MCU). The transmitter of the QAM signal was a Keysight M8190A arbitrary waveform generator (AWG) and the receiver was a Keysight N9030A signal analyzer. The system was calibrated with SMA cables to maintain identical amplitude ratios between states 1 and 2; a phase shifter was used to keep both signals in-phase at the receiver. The measurement test setup is described fully in Fig. 1(b).

The MCU provided switching signals with rise time

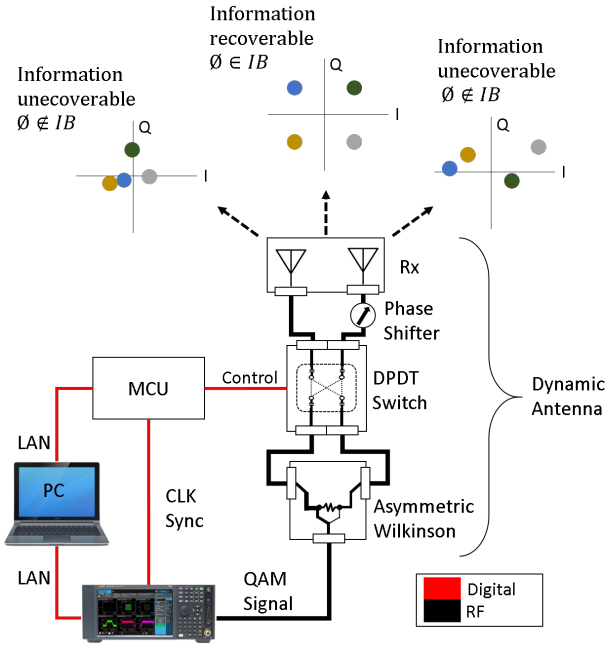

Fig. 1. Experimental setup used to evaluate the secure wireless operation of the dynamic antenna array. Note that beamsteering can be obtained using additional element-level phase shifters and standard phased array element weighting.

$\tau_r = 5$ ns, duration $\tau = 0.5$ μs, signal amplitude $A = 3.3$ V and switching period $T_0 = 1$ μs. Rapidly switched signals may generate interference; here we characterize the spurious signals generated by the waveform. The spectral envelope of a trapezoidal pulse train can be given by [16]

$$\text{env} = 2A\frac{\tau}{T_0}\left|\text{sinc}\left(\pi\tau f\right)\right|\left|\text{sinc}\left(\pi\tau_r f\right)\right| \tag{5}$$

where f is the frequency in Hz. In a 50 Ω system, the power generated by the MCU signal is a maximum –100 dBm around 2.5 GHz, which is below the measured noise floor of –95 dBm. The RF switch can support a rise time of $\tau_r = 35$ ns; with this, a maximum input power of 32 dBm, and the remaining parameters the same as the control signal, the maximum power from the switch would be –99.6 dBm around 2.5 GHz. For both switching signals, the maximum values of the envelopes at frequencies near 2.5 GHz are below the noise floor of –95 dBm, thus the signals will be unaffected. The switch also has a 2nd and 3rd order harmonic mitigation of –70 dBc to further mitigate spurious signals. Mitigation of signals from Wi-Fi and external sources was taken into account by taking measurements in an unoccupied spectrum around 2.5 GHz.

III. Experimental Results

Experimental measurements were conducted in a semi-enclosed anechoic range spanning 7.6 m. A polystyrene pedestal on a rotator stage with 1° accuracy positioned the antenna under test. The measurements were conducted in the far field at a height of approximately 125 cm and a radial distance of 225 cm. Bit error ratio (BER) measurements were recorded in 1° increments over the front half ϕ-plane $\phi \in [-90, 90]°$. The transmitter antenna was an L-Com

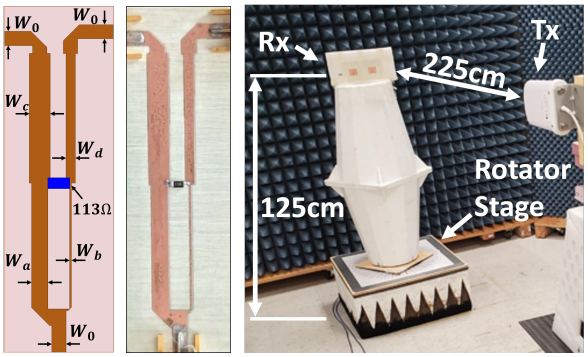

Fig. 2. Asymmetric Wilkinson power divider model (left) and manufactured device (center). Trace widths: $W_0 = 3.273$ mm, $W_a = 3.803$ mm, $W_b = 0.408$ mm, $W_c = 4.775$ mm, $W_d = 2.127$ mm. The lengths of the W_0 traces are 10 mm and the a/b/c/d trace lengths are 30 mm. A 113Ω resistor is used to isolate the ports. (Right) Photograph of the measurement system in the lab showing the dynamic antenna mounted to a foam board in a semi-anechoic environment.

HG2458-08LP-NF log-periodic antenna transmitting a 16-QAM constellation single carrier at a rate of 4 Mbits/s. The receiving dynamic antenna system was mounted to a polystyrene structure with an element spacing of 0.75λ, as shown in Fig. 2. The received signal-to-noise ratio (SNR) was 33 dB, which ensured that any errors seen at the receiver would be due solely to directional modulation from antenna dynamics, and not due to low SNR.

The BER was measured as a function of angle in both static cases, state 1 and 2, as well as the dynamic switching state. Both state 1 and 2 yielded similar results of having perfect data transmission across the 181 angles of measurement, thus in the static cases BER = 0. This ensured that the SNR was sufficiently high so that low-amplitude signals (e.g., near the nulls of the antenna pattern) would not cause any errors in the dynamic switching antenna. The measured BER as a function of angle for the dynamic antenna is shown in Fig. 3. The simulated BER is also shown for two cases: the ideal model simulated in MATLAB with isotropic antenna patterns using (1), and the simulated BER using the complex antenna pattern generated from HFSS. It is clear that the dynamic antenna generates sufficient additional signal modulation to degrade the information at angles outside of a narrow region near broadside. The static cases yielded no errors in all directions. The proposed dynamic antenna thus yields an information beamwidth (where information is recoverable) of approximately ±13°, while in a static state the antenna yielded no errors at all angles.

The measured BER is similar to that modeled in MATLAB using isotropic and HFSS-generated radiation patterns, but with a slightly wider information beamwidth. This may be due partly to manufacturing tolerances of the two patch antennas resulting in slight asymmetries in the element gain pattern and phase pattern characteristics. Furthermore, the calibration did not correct for any amplitude mismatch between the two elements, which may alter the amplitude ratio. Despite these non-idealities, the proposed dynamic antenna nonetheless generated a narrow window where information can be transmitted securely, while the static design allowed

TABLE I
DM SYSTEM PERFORMANCE COMPARISON

Literature	SNR (dB)	IB_{sim}	IB_{meas}	Symbols	Elements	Switches	Footprint
This work	**33**	**14**	**26**	**16**	**2**	**1**	**0.75**λ
[10]	12	~	13	4	4	0	2.00λ
[12]	30	112	25	16	1	4	1.50λ
[11]	12	5	5	2	2	0	4.70λ
[7]	12	5	~	4	2	0	0.50λ
[8]	10	50	~	2	8	8	3.50λ
[5]	15	7	~	4	5	0	2.00λ
[6]	∞	10	~	4	5	0	2.00λ
[4]	∞	2	~	210	1	90	0.30λ

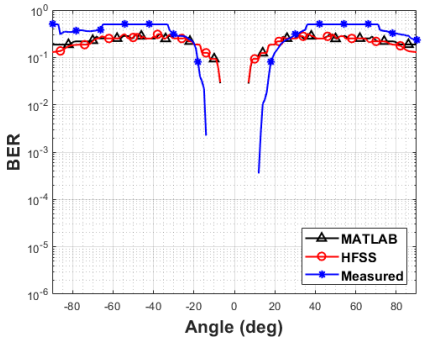

Fig. 3. Simulated and measured bit error ratios (BERs) showing low errors only in the broadside direction. The static antenna measurements yielded zero BER in all directions, indicating high SNR in all measurements, and thus the errors were due solely to the antenna array dynamics.

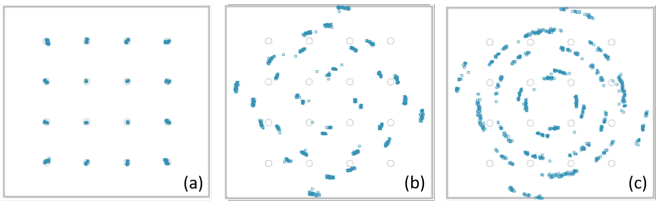

Fig. 4. Constellation diagram of 16-QAM communication with spatial amplitude modulation at (a) 0° (b) −30° and (c) 30°, showing the effect of the additional modulation imparted by the dynamic antenna array. Unfilled circles indicate the desired symbol locations, while filled circles indicate the measured symbols. At broadside (a) the 16-QAM data is tightly clustered and easily demodulated. In (b) and (c) the signals away from broadside exhibit high SNR, indicated by the close clustering of the information; however, the additional modulation from the antenna corrupts the amplitude at a small scale and the phase significantly, preventing correct demodulation. Since the SNR is high, the reduction in BER at angles away from broadside is due only to the antenna dynamics.

zero BER in all directions.

Constellation diagrams were measured at various angles to demonstrate the impact of the dynamic array on received data. Fig. 4 shows the constellation diagrams of the data transmitted at three representative angles: broadside to the dynamic array (0°), where the radiation pattern is static, and at two angles to the side (±30°), where the pattern is dynamic. Fig. 4(a) shows the correct constellation at broadside, with high SNR and tight clustering of the symbols. Figs. 4(b) and 4(c) show the constellations at ±30°. It is clear that the SNR is still high due to the clustering of the information; however, because of the additional modulation imparted by the antenna dynamics the information is misaligned in amplitude at an appreciable level, and misaligned in phase significantly, preventing correct demodulation. Since the SNR is high, the degradation in the signal is due only to the antenna dynamics. The impacts on information throughput at angles away from the mainbeam are due principally to phase dynamics in the presented antenna; however, if the amplitude dynamics are enhanced, additional reductions in the size of the information beamwidth can be obtained [12]. A comparison to prior work is shown in Table I; measured values are listed for systems where communications signals were measured. The number of symbols in the waveform is included, since it is harder to achieve DM in waveforms with fewer symbols. IB_{sim} and IB_{meas} are the information beamwidth where a BER $< 10^{-3}$.

IV. CONCLUSION

In this work, we presented a novel dynamic two-element antenna to achieve directional modulation for secure wireless communications. It was shown that with limited RF hardware, sufficient communication security can be demonstrated by obtaining a high BER outside of a narrow information beamwidth, $\phi \leq |13°|$, in a nearly noiseless environment. The proposed approach relies on additional hardware elements, however the power consumption of the switches will be marginal, and little knowledge of the underlying communications system is necessary. Furthermore, the information beamwidth can directly be steered using standard array phase shifting. The proposed dynamic system implements wireless security at the physical layer, and furthermore can be implemented in a “black box” fashion that is transparent to the rest of the communications system. Thus, it may be used as an additional layer of security in future wireless systems or may be used in existing systems with minimal reconfiguration. Furthermore, a brief comparison of DM techniques in this work and past literature can help the reader quickly assess the unique demands to their application through various metrics. Spurious signals are also explained briefly and methods to analyze and mitigate them.

ACKNOWLEDGMENT

This work was supported in part by the National Science Foundation under Grant #2028736. The authors thank Skyworks Solutions for the DPDT RF switch, and C. Hilton and O. Ramachandran, Michigan State University, for helpful discussions.

REFERENCES

[1] Y. Zou, J. Zhu, X. Wang, and L. Hanzo, "A survey on wireless security: Technical challenges, recent advances, and future trends," *Proceedings of the IEEE*, vol. 104, no. 9, pp. 1727–1765, 2016.

[2] C. Miller and C. Valasek, "Securing self-driving cars (one company at a time)," *Black Hat*, 2018.

[3] P. Kapoor, A. Vora, and K.-D. Kang, "Detecting and mitigating spoofing attack against an automotive radar," in *2018 IEEE 88th Vehicular Technology Conference (VTC-Fall)*, 2018, pp. 1–6.

[4] A. Babakhani, D. B. Rutledge, and A. Hajimiri, "Transmitter architectures based on near-field direct antenna modulation," *IEEE Journal of Solid-State Circuits*, vol. 43, no. 12, pp. 2674–2692, 2008.

[5] B. Guo, Y.-h. Yang, G. Xin, and Y.-q. Tang, "Combinatorial interference directional modulation for physical layer security transmission," in *2016 IEEE Information Technology, Networking, Electronic and Automation Control Conference*, 2016, pp. 710–713.

[6] Y. Ding and V. F. Fusco, "A vector approach for the analysis and synthesis of directional modulation transmitters," *IEEE Transactions on Antennas and Propagation*, vol. 62, no. 1, pp. 361–370, 2014.

[7] S. Mufti, J. Parrón, and A. Tennant, "Hardware implementation of directional modulation system with a 2 element antenna array," in *2017 11th European Conference on Antennas and Propagation (EUCAP)*, 2017, pp. 3239–3242.

[8] Q. Zhu, S. Yang, R. Yao, and Z. Nie, "A directional modulation technique for secure communication based on 4d antenna arrays," in *2013 7th European Conference on Antennas and Propagation (EuCAP)*, 2013, pp. 125–127.

[9] M. P. Daly and J. T. Bernhard, "Directional modulation technique for phased arrays," *IEEE Transactions on Antennas and Propagation*, vol. 57, no. 9, pp. 2633–2640, 2009.

[10] M. P. Daly, E. L. Daly, and J. T. Bernhard, "Demonstration of directional modulation using a phased array," *IEEE Transactions on Antennas and Propagation*, vol. 58, no. 5, pp. 1545–1550, 2010.

[11] S. M. Ellison, J. M. Merlo, and J. A. Nanzer, "Distributed antenna array dynamics for secure wireless communication," *IEEE Transactions on Antennas and Propagation*, vol. 70, no. 4, pp. 2740–2749, 2022.

[12] A. A. Arisheh, J. M. Merlo, and J. A. Nanzer, "Design of a single-element dynamic antenna for secure wireless applications," *IEEE Transactions on Antennas and Propagation*, pp. 1–1, 2023.

[13] E. Baghdady, "Directional signal modulation by means of switched spaced antennas," *IEEE Transactions on Communications*, vol. 38, no. 4, pp. 399–403, 1990.

[14] L. Parad and R. Moynihan, "Split-tee power divider," *IEEE Transactions on Microwave Theory and Techniques*, vol. 13, no. 1, pp. 91–95, 1965.

[15] B. C. Wadell, *Transmission line design handbook*. Artech House Microwave Library, 1991.

[16] C. R. Paul, R. C. Scully, and M. A. Steffka, *Introduction to electromagnetic compatibility*. John Wiley & Sons, 2022.